

RESEARCH

Open Access



Associations of choroid plexus volume with white matter hyperintensity volume and susceptibility and plasma amyloid markers in cerebral small vessel disease

Pengcheng Liang^{1†} , Meng Li^{2†}, Yiwen Chen¹, Zhenyu Cheng³, Na Wang¹, Yuanyuan Wang³, Nan Zhang¹, Yena Che¹, Jing Li^{4*} , Changhu Liang^{1*}  and Lingfei Guo^{1*} 

Abstract

Background White matter hyperintensity (WMH) is a key feature of cerebral small vessel disease (CSVD). The impact of the choroid plexus (CP) volume on disease progression remains largely unexplored. This study evaluated the relationship between CP volume and CSVD severity via WMH volume and susceptibility values. Additionally, we explored whether Alzheimer's disease (AD)-related plasma proteins influence the volume of the CP.

Methods and materials Our study included 291 CSVD individuals, with 84 participants completing subsequent brain MRI at a mean follow-up of 20 months. To explore the potential CP-associated pathways, we assessed the relationships between AD-related plasma biomarkers and CP volume via multiple linear regression analysis. The longitudinal associations between CP volume and WMH characteristics (WMH volume and susceptibility) were analyzed via linear mixed-effects models. Finally, we employed random forest analysis with the Boruta algorithm to identify key predictors of CSVD severity.

Results Plasma A β 1–40 levels were positively correlated with CP volume ($\beta=0.115$, $P=0.009$), whereas A β 42–40 ratio were negatively associated with CP volume ($\beta=-0.135$, $P=0.03$). Notably, increased CP volume was associated with both greater WMH burden ($\beta=0.191$, $P=0.011$) and decreased WMH susceptibility ($\beta=-0.192$, $P=0.012$). Furthermore, random forest modeling identified CP volume and WMH susceptibility as the strongest predictors of CSVD severity.

Conclusions CP volume changes were significantly correlated with both WMH volume and WMH susceptibility in CSVD patients. These findings suggest that CP-mediated pathways may link amyloid metabolism to CSVD progression.

[†]Pengcheng Liang and Meng Li contributed equally to this work and are co-first authors.

*Correspondence:

Jing Li
lja04485@btch.edu.cn
Changhu Liang
tigerlch@163.com
Lingfei Guo
glfsci@163.com

Full list of author information is available at the end of the article



Keywords Cerebral small vessel disease, White matter hyperintensities, Choroid plexus volume, Quantitative susceptibility mapping, Amyloid-beta

Introduction

Cerebral small vessel disease (CSVD) has emerged as a significant health challenge among aging populations globally, contributing to cognitive impairment, increased incidence of stroke, and disability [1, 2]. White matter hyperintensities (WMHs), recognized as pivotal imaging indicators of CSVD, are closely linked to unfavorable clinical outcomes, such as cognitive dysfunction and increased stroke risk [3, 4]. Recent investigations underscore the critical role of cerebrospinal fluid (CSF) homeostasis in preserving the structural and functional integrity of white matter [5]. As the main source of CSF production, the choroid plexus (CP) influences WMH progression by regulating both CSF homeostasis and neuroinflammatory responses [6].

Recent studies have shown a relationship between changes in CP volume and neurodegenerative disorders [6]. Investigations focusing on Alzheimer's disease (AD) have revealed that CP enlargement is correlated with increased CSF inflammatory marker levels [7], potentially reflecting alterations in CSF dynamics and brain clearance mechanisms [8]. These CP-related changes are hypothesized to exacerbate disease progression by disrupting CSF dynamics and hindering the clearance of neurotoxic substances [8]. Although extensive studies have established the involvement of the CP in neuroinflammation and blood–brain barrier function, its specific contributions to the pathogenesis of CSVD remain ambiguous. A pivotal question to address is whether variations in CP volume reflect the severity of CSVD by influencing the structural integrity and microarchitecture of WMH.

While WMH volume has long been recognized as a conventional marker for evaluating the severity of CSVD, its ability to capture subtle alterations in white matter microstructure through volume analysis alone remains limited [9]. Advances in neuroimaging techniques, particularly quantitative susceptibility mapping (QSM), offer a transformative approach by enabling precise characterization of tissue properties, such as myelin integrity and iron distribution [10]. By integrating volume measurements with susceptibility-based analysis, researchers can gain deeper insights into the underlying mechanisms of white matter pathology. The combined methodology holds significant potential for identifying early indicators of disease progression, even before detectable volume changes occur.

Emerging evidence highlights the pivotal role of amyloid-beta ($A\beta$) proteins, particularly $A\beta_{1-40}$, $A\beta_{1-42}$, and their ratio ($A\beta_{42/40}$), as key regulators in the pathophysiology of neurodegenerative disorders [11]. The relationship between amyloid-beta proteins and cerebral small vessel disease remains complex and not fully understood. Previous research investigating this relationship has yielded inconsistent results. A comprehensive systematic review examining the associations between amyloid- β and white matter hyperintensities across 42 studies revealed substantial heterogeneity in findings. While some studies reported positive correlations between amyloid burden and WMH severity, others found no significant associations, and a few even suggested inverse relationships [12]. Similarly, investigations into interactions between brain amyloid- β , CSVD markers, and cognitive function demonstrated that while both pathologies independently affected cognition, there was limited evidence for synergistic effects between amyloid burden and CSVD markers [13]. These inconsistencies might stem from methodological differences, sample heterogeneity, or an overreliance on conventional volumetric measurements alone. We propose that incorporating advanced neuroimaging techniques, particularly QSM of white matter hyperintensities, may provide deeper insights into tissue microstructural changes that volumetric analysis cannot capture. QSM offers valuable information about tissue composition, including myelin integrity and iron distribution, potentially revealing subtle relationships between amyloid metabolism and CSVD pathology. Dysfunction of the CP has been implicated in cerebrovascular health deterioration, potentially driven by the abnormal accumulation of these proteins [7, 14]. While the connection between $A\beta$ proteins and CP alterations has been extensively studied in AD, their contributions to CSVD-related white matter damage via CP-mediated pathways remain insufficiently understood [13]. Investigating the interplay among plasma $A\beta$ levels, CP volume, and WMH characteristics (WMH volume and susceptibility) may reveal shared pathological mechanisms underlying AD and CSVD. While CSVD has traditionally been viewed as a purely vascular condition, growing evidence suggests overlap between vascular and neurodegenerative pathways. Recent studies have shown that tau pathology may be influenced by vascular dysfunction, and elevated tau levels have been associated with white matter damage in various contexts.

Therefore, we included tau markers to explore potential mechanistic links between vascular injury and neurodegeneration in CSVD.

In this study, we investigated the relationships between CP volume, WMH characteristics (WMH volume and susceptibility), and AD-related plasma proteins in CSVD participants using advanced MRI techniques. By performing both cross-sectional and longitudinal analyses over a 20-month observation period, we evaluated the associations between CP volume dynamics and WMH progression. QSM was integrated with traditional volumetric assessments to provide a more comprehensive characterization of white matter alterations. Additionally, machine learning techniques were applied to pinpoint critical predictors of CSVD severity across the parameters measured. By combining multimodal imaging and plasma biomarker analyses, this study investigated the pivotal role of the CP in CSVD pathophysiology,

shedding light on its connections to neurodegeneration and cerebrovascular pathological processes.

Methods

Study participants

This prospective study was approved by the Institutional Review Board of Shandong Provincial Hospital Affiliated with Shandong First Medical University. All participants provided written informed consent before enrollment. Among the 554 participants recruited from January 2021 to December 2023, 291 were included in the final analysis (Fig. 1). The diagnosis of CSVD was based on established neuroimaging criteria, including the presence of recent small subcortical infarcts, lacunes of presumed vascular origin, white matter hyperintensities, enlarged perivascular spaces, cerebral microbleeds, cortical superficial siderosis, brain atrophy, or cortical cerebral microinfarcts [10] (Fig. 2a).

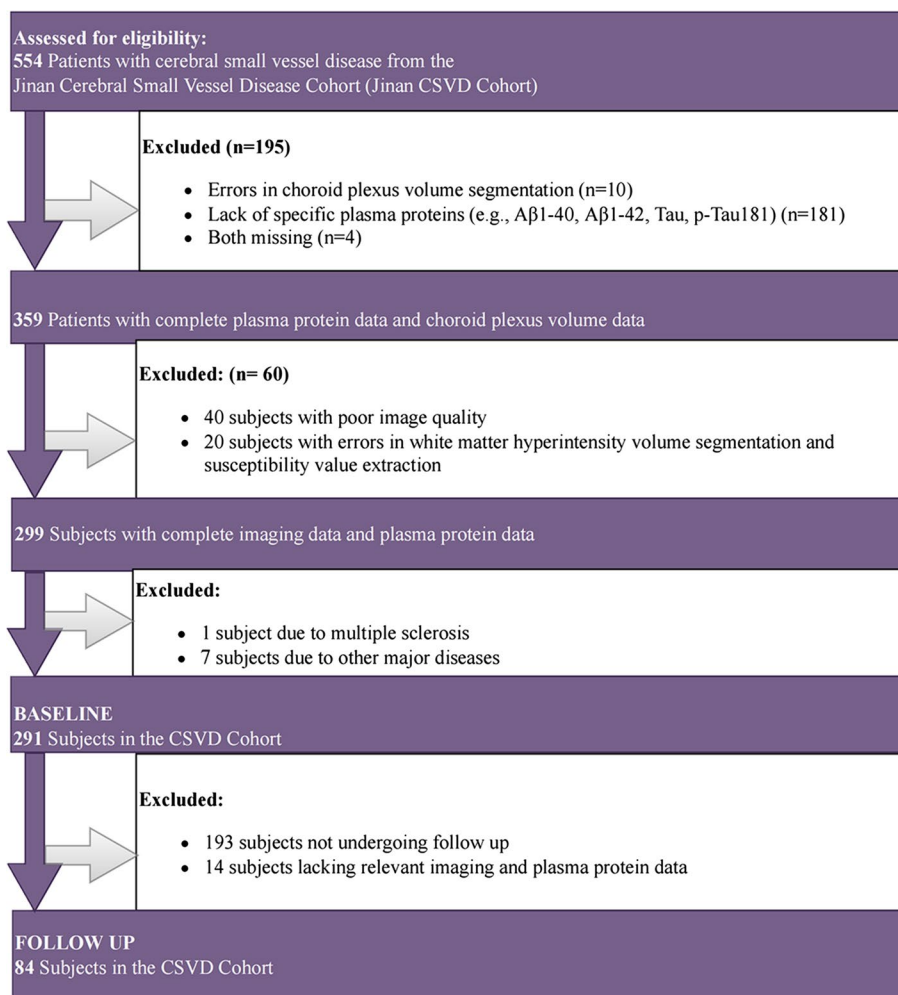


Fig. 1 Flowchart of participant selection. Abbreviations: CSVD = cerebral small vessel disease

CSVD severity was evaluated using a comprehensive scoring system that assesses the total burden of small vessel disease [15, 16]. Specifically, one point was assigned for each of the following: presence of ≥ 1 lacunar infarct; early confluent deep WMH (Fazekas score [17] 2 or 3) or irregular periventricular WMH extending into deep white matter (Fazekas score 3); moderate to severe (grade 2–3) enlarged perivascular spaces in the basal ganglia; and presence of ≥ 1 cerebral microbleed. On the basis of these criteria, the participants were stratified into three groups: CSVD(0) ($n = 194$, total score of 0), CSVD(1) ($n = 50$, total score of 1), and CSVD(2) ($n = 47$, total score of 2–4).

The exclusion criteria included the following: (1) the presence of organic brain lesions (e.g., stroke, tumors, trauma); (2) a history of psychiatric or neurological disorders affecting cognitive function; (3) a history of alcohol or substance abuse; (4) acute complications of type 2 diabetes; (5) severe organ dysfunction; (6) severe hypertension; and (7) significant visual or auditory impairment that could interfere with assessment. While participants with dementia, Parkinson's disease, or other major neurological disorders that could significantly impact cognitive function were excluded, our study included cognitively unimpaired individuals as well as those with milder cognitive changes that can be associated with CSVD.

Imaging acquisition protocol

All participants underwent MRI examination on a 3.0-T Siemens medical system (Erlangen, Germany) equipped with a 32-channel head coil for signal reception. Three-dimensional T1-weighted (3D T1 W) structural images were obtained using the Magnetization Prepared Rapid Gradient Echo (MPRAGE) sequence with the following parameters: Repetition Time (TR) = 7.3 ms; Echo Time (TE) = 2.4 ms; Inversion Time (TI) = 900 ms; Flip Angle = 9°; Isotropic voxel size = 1 mm³. For quantitative susceptibility measurements, a 3D multi-echo gradient echo (mGRE) sequence was performed with TR = 50 ms, first TE = 6.8 ms, TE interval = 4.1 ms, number of echoes = 10, flip angle = 15°, and voxel size = 1 × 1 × 2 mm³. Additionally, T2-weighted fluid attenuated inversion recovery

(FLAIR) and T2-weighted turbo spin echo sequences were acquired to identify cerebral abnormalities.

Image postprocessing

The structural MRI data were preprocessed via fMRIPrep 20.1.1, which generated a nonlinear deformation field mapping native space to the MNI2009c space [18]. WMH segmentation was performed using an optimized algorithm based on Multidimensional Gated Recurrent Units, incorporating data augmentation, selective sampling, residual learning, and DropConnect in the RNN state [19]. The algorithm utilized T1 W and FLAIR images to generate WMH masks in native T1 W space. Manual correction of segmentation inaccuracies was performed for each participant, followed by algorithm parameter updates and rerun until accurate segmentation was visually confirmed. WMH volumes were subsequently extracted using fsstats (Fig. 2b).

Additionally, the CAT12 toolbox (Computational Anatomy Toolbox 12, version 12.8_1977), implemented in Statistical Parametric Mapping (SPM12, r7771), was employed to generate GM/WM/CSF masks in native space. These masks, combined with WMH segmentation, facilitated the extraction of average susceptibility values from both WMH and non-WMH white matter regions (Fig. 3).

The choroid plexus was segmented from 3D-T1-weighted images using a deep learning algorithm based on 3D nnU-Net. The algorithm was developed and validated in a cohort of 630 CSVD patients, with CP regions initially labeled by two experienced radiologists (with 7 and 20 years of experience). A senior radiologist with 25 years of expertise performed manual visual inspection and necessary adjustments for quality control. The model was trained on 420 randomly selected cases and tested on the remaining 210 cases (Dice score = 0.8; $P < 0.001$). After application to the current study cohort, all automated segmentation results were evaluated and approved by an additional senior radiologist who was blinded to the clinical information.

QSM images were normalized using CSF as a reference, which was achieved by dividing voxel values by the average susceptibility in the lateral ventricle region. CP

(See figure on next page.)

Fig. 2 Overview of methodology **a** CSVD severity was evaluated via four established neuroimaging markers on 3 T MRI: white matter hyperintensities, lacunes, enlarged perivascular spaces, and cerebral microbleeds. **b** Our research focused on two main aspects: plasma biomarkers and brain imaging characteristics. For plasma biomarkers, we measured A β 40, A β 42, and A β 42/40. The results of the brain imaging analysis included WMH volume, WMH susceptibility, and choroid plexus volume. **c** Statistical analysis was conducted in multiple steps. First, linear regression models were used to analyze the relationships between plasma biomarkers and CP volume. Second, regression analysis was used to examine associations between CP volume and white matter characteristics (WMH volume and susceptibility). Finally, linear mixed-effects models were employed to assess the longitudinal relationships between CP volume and WMH measurements. Abbreviations: CSVD = cerebral small vessel disease; CP = choroid plexus; WMH = white matter hyperintensity

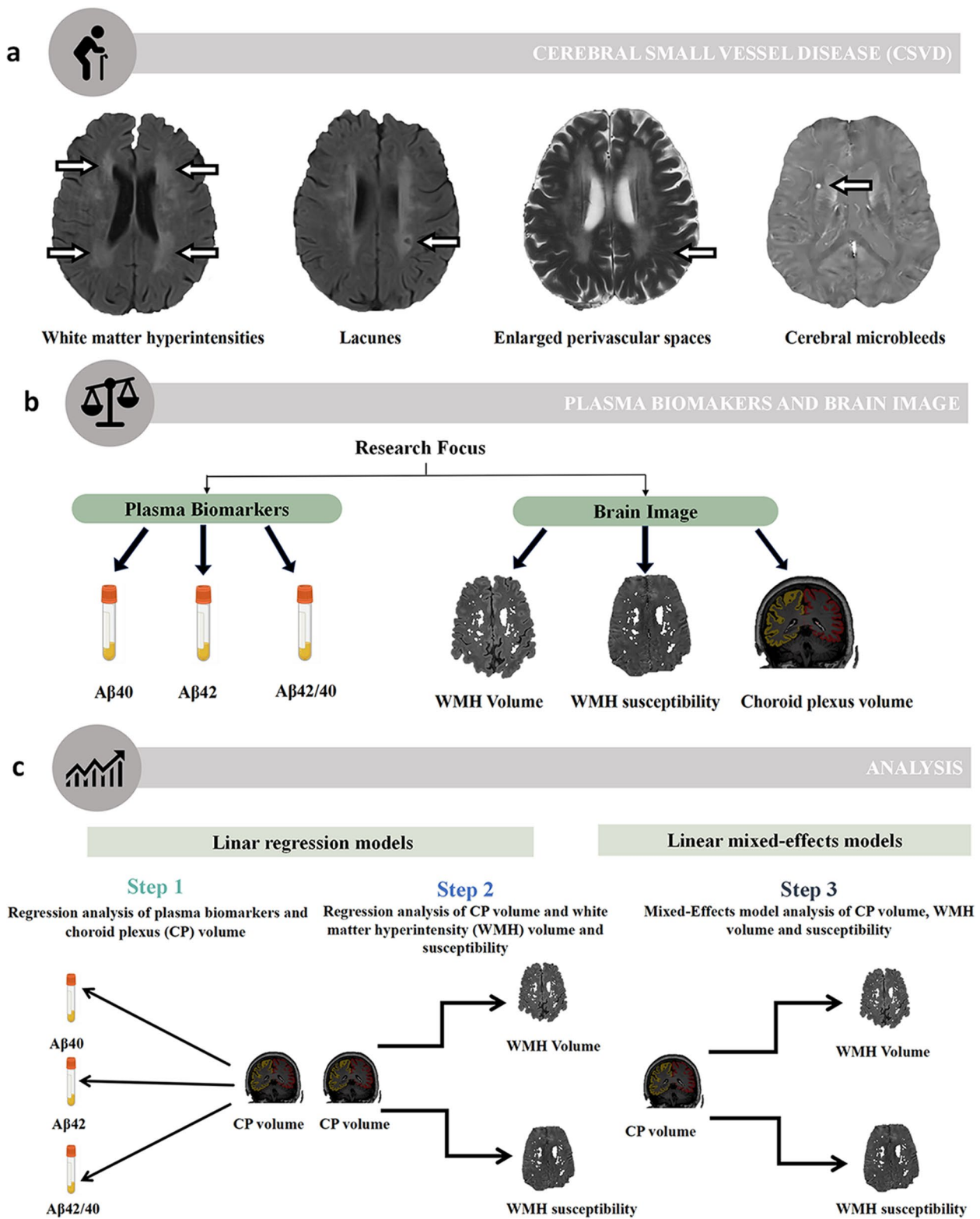


Fig. 2 (See legend on previous page.)

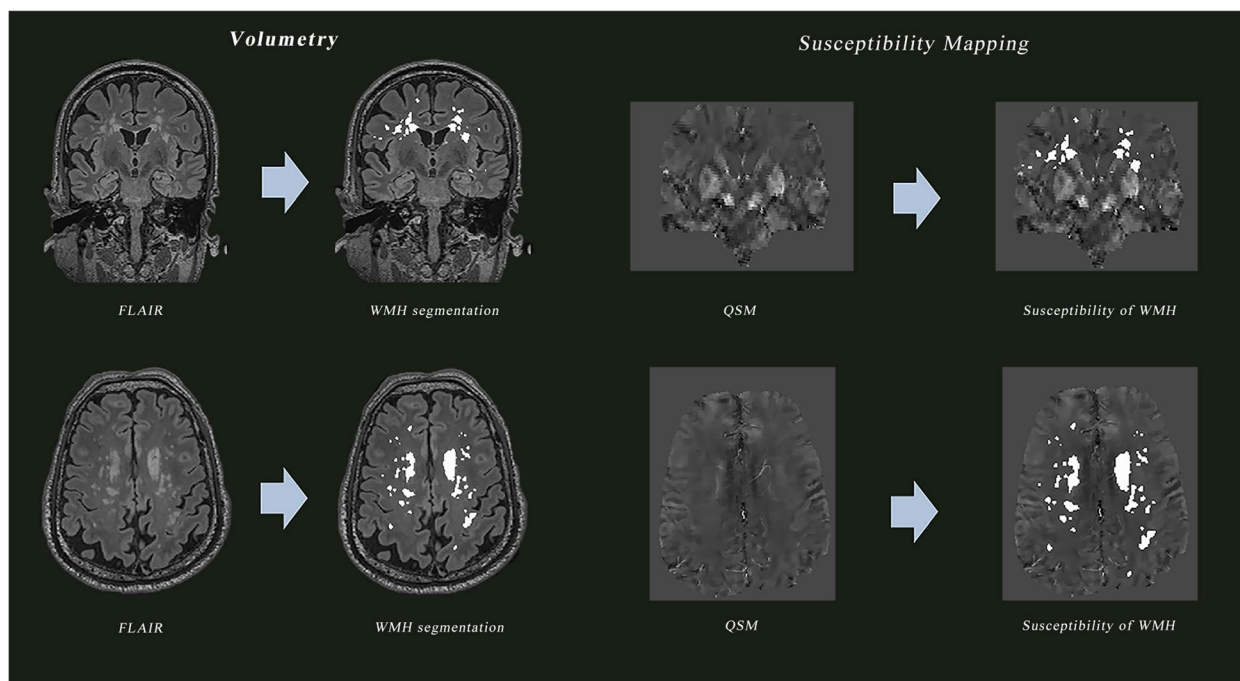


Fig. 3 MRI processing steps. To obtain the WMH mask, we applied the algorithm developed by Andermatt et al., which employs Multidimensional Gated Recurrent Units with optimizations including data augmentation, selective sampling, residual learning, and DropConnect in the RNN state. This algorithm utilized T1 and FLAIR images to generate the WMH mask in the native T1 space. Additionally, the CAT 12 toolbox (Computational Anatomy Toolbox 12, version 12.8_1977), implemented in Statistical Parametric Mapping (SPM12, r7771, Wellcome Trust Centre for Neuroimaging, University College London), was used to generate GM/WM/CSF masks in native space for each participant. The derived WMH and WM masks facilitated the extraction of the average susceptibility value within WMH and nonWMH WM voxels. Abbreviations: WMH = white matter hyperintensity

susceptibility values were obtained by overlaying the CP mask onto the normalized QSM image, following coregistration of CP segmentation from the T1-weighted space to the QSM space.

Laboratory measurements

Plasma samples were obtained through venipuncture via standardized collection protocols. Five milliliters of venous blood were collected in EDTA tubes, followed by centrifugation at 3000 rpm for 15 min. The separated plasma was initially aliquoted and stored at -20°C , with long-term preservation at -70°C .

Plasma levels of $\text{A}\beta_{1-42}$ and $\text{A}\beta_{1-40}$ were measured using enzyme-linked immunosorbent assay (ELISA) kits specific for human proteins (Thermo Fisher/Invitrogen, United States). To ensure measurement consistency, all samples were processed using a single reagent batch according to manufacturer protocols.

In addition to $\text{A}\beta_{1-42}$ and $\text{A}\beta_{1-40}$, plasma levels of total tau and phosphorylated tau at threonine 181 (p-tau181) were also measured using the same ELISA platform (Thermo Fisher/Invitrogen, United States) following identical protocols. All tau measurements were

performed in the same batch as the amyloid markers to ensure consistency across all biomarker analyses.

Statistical analysis

For plasma biomarker analyses, data normality was assessed via the Kolmogorov–Smirnov test. Plasma biomarkers ($\text{A}\beta_{1-40}$, $\text{A}\beta_{1-42}$, and $\text{A}\beta_{42/40}$) were log-transformed and standardized to Z scores to meet normality assumptions. Associations between plasma markers and CP/ICV (intracranial volume) were examined using multiple linear regression models. The models were adjusted for the following demographic factors: age, sex, and educational level. False discovery rate (FDR) correction was applied for multiple comparisons.

Multiple linear regression models were employed to examine associations between CP volume and WMH characteristics (WMH volume and susceptibility) (Fig. 2c). CP volume served as the independent variable, whereas WMH volume and WMH susceptibility values were analyzed as separate dependent variables. The models were adjusted for age, sex, educational level, and bilateral ventricular volume.

Linear mixed-effects models were utilized to investigate the relationships between CP volume and WMH measurements. These models incorporated CP volume as the independent variable, with either WMH volume or WMH susceptibility values as the dependent variable. Fixed effects included age, sex, bilateral ventricular volume, and follow-up time. Random intercepts were included to account for subject-specific variations.

To evaluate the relative importance of multiple predictors in explaining CSVD severity, we employed random forest models with the Boruta algorithm for feature selection. The algorithm conducted 2,000 iterations, comparing the importance of original features against randomly generated shadow attributes and using multiple comparison-adjusted binomial tests to ensure statistical significance. Random forest models were constructed with 10,000 trees to ensure robust feature selection.

To explore direct relationships between plasma amyloid markers and WMH characteristics, we conducted additional regression analyses examining associations between plasma A β markers (A β 1–40, A β 1–42, and A β 42/40) and both WMH volume and WMH susceptibility. These models were adjusted for age, gender, educational level, diabetes, and hypertension.

A two-sided P value <0.05 was considered statistically significant. Statistical analyses were performed via IBM SPSS Statistics (version 26.0, IBM Corp., Armonk, NY, USA) and R software (version 4.3.2, R Foundation for Statistical Computing, Vienna, Austria).

Results

Baseline characteristics of study population

A total of 291 participants with varying degrees of CSVD severity were enrolled in this study. The participants were categorized into three groups according to severity: CSVD(0) ($n = 194$), CSVD(1) ($n = 50$), and CSVD(2) ($n = 47$). Table 1 summarizes the baseline demographic characteristics, medical history, plasma biomarkers, and neuroimaging parameters across groups. Neuroimaging analysis revealed that both the CP volume and the CP/ICV ratio were significantly greater in the CSVD(2) group than in the CSVD(0) and CSVD(1) groups (all $P < 0.001$). Furthermore, significant differences in WMH volume and WMH susceptibility were observed among the three groups (all $P < 0.001$).

Table 1 Demographic and MRI characteristics of analyzed study sample

Variables	CSVD(0) ($n = 194$)	CSVD(1) ($n = 50$)	CSVD(2) ($n = 47$)	F/ χ^2 /K	P-value
Demographics					
Age (years, mean \pm SD)	57.43 \pm 8.53	62.22 \pm 7.17	64.02 \pm 8.33	16.177	< 0.001
Sex [female, n (%)]	116 (59.79)	26 (52.00)	20 (42.55)	4.89	0.087
Education (median, IQR)	16.00 (12.00, 18.00)	12.00 (9.00, 15.00)	12.00 (9.00, 15.00)	38.95	< 0.001
Medical history					
Hypertension [yes, n (%)]	45 (23.20)	23 (46.00)	32 (68.09)	38.94	< 0.001
Diabetes [yes, n (%)]	50 (25.77)	20 (40.00)	25 (53.19)	16.29	< 0.001
Hyperlipidemia [yes, n (%)]	65 (33.51)	22 (44.00)	23 (48.94)	4.16	0.125
Smoking [yes, n (%)]	30 (15.46)	13 (26.00)	10 (21.28)	3.32	0.191
Drinking [yes, n (%)]	48 (24.74)	15 (30.00)	17 (36.17)	2.67	0.263
Plasma biomarkers					
A β 42 [pg/L, median (IQR)]	5.13 (4.96, 5.31)	5.13 (4.99, 5.30)	5.15 (4.87, 5.25)	1.37	0.504
A β 40 [pg/L, median (IQR)]	5.55 (5.30, 5.72)	5.56 (5.24, 5.70)	5.63 (5.19, 5.77)	0.87	0.647
A β 42/40 [median (IQR)]	0.51 (0.44, 0.63)	0.54 (0.39, 0.69)	0.49 (0.43, 0.57)	1.51	0.471
Neuroimaging measures					
CP Volume [mm ³ , median (IQR)]	1131.94 (849.55, 1406.42)	1335.63 (1173.67, 1576.69)	1494.23 (1291.34, 1730.74)	33.14	< 0.001
CP/ICV [$\times 10^{-3}$, median (IQR)]	0.77 (0.57, 0.96)	0.94 (0.76, 1.13)	0.98 (0.82, 1.20)	31.38	< 0.001
Mean QSM WMH [ppb $\times 10^{-9}$, median (IQR)]	– 19.18 (– 25.49, – 12.10)	– 14.98 (– 20.13, – 9.59)	– 10.81 (– 15.46, – 4.48)	32.05	< 0.001
Left Ventricle Volume [mm ³ , median (IQR)]	7740.10 (5619.20, 11,156.65)	11,058.40 (8351.80, 13,800.70)	14,351.35 (9548.77, 19,204.30)	45	< 0.001
Right Ventricle Volume [mm ³ , median (IQR)]	7069.20 (4781.85, 9635.60)	9833.50 (7181.50, 12,300.00)	13,596.40 (8610.48, 16,628.25)	45.41	< 0.001
WMH Volume [mm ³ , median (IQR)]	283.97 (124.19, 687.00)	925.49 (560.43, 2252.81)	4325.27 (2584.64, 9036.96)	116.81	< 0.001

Abbreviations CSVD Cerebral small vessel disease, CP/ICV Choroid plexus volume normalized to intracranial volume, WMH White matter hyperintensity

Impact of AD-related plasma proteins on CP volume

To examine the relationship between amyloid-beta plasma biomarkers and CP volume, we analyzed three key measurements: A β 1–40, A β 1–42, and A β 42/40. After FDR correction for multiple comparisons, linear regression analysis revealed a significant positive correlation between A β 1–40 levels and CP/ICV ($\beta = 0.115$, $P = 0.009$). The A β 42/40 ratio was significantly negatively associated with the CP/ICV ($\beta = -0.135$, $P = 0.03$) (Fig. 4). In contrast, no significant associations were detected between A β 1–42 and CP/ICV ($\beta = -0.011$, $P = 0.836$).

Direct associations between plasma amyloid markers and WMH characteristics

To explore potential relationships between amyloid markers and white matter changes, we analyzed the direct associations between plasma amyloid markers and WMH characteristics (Table S 1). After adjusting for age, gender, educational level, diabetes, and hypertension, we found that the A β 42/40 ratio was positively associated with WMH susceptibility ($\beta = 0.13$, $P = 0.040$). No significant associations were observed between other plasma amyloid markers (A β 1–40, A β 1–42) and WMH susceptibility. Additionally, none of the examined plasma amyloid markers showed significant associations with WMH volume.

Cross-sectional and longitudinal relationships between CP volume and WMH characteristics (WMH volume and susceptibility)

After adjusting for potential confounders, our cross-sectional analysis revealed significant associations between CP volume and both WMH volume and susceptibility values. Specifically, regression analysis revealed that greater CP volume was significantly associated with greater

WMH volume ($\beta = 0.191$, $P = 0.011$) and reduced WMH susceptibility values ($\beta = -0.192$, $P = 0.012$) (Fig. 5).

Longitudinal analysis using linear mixed-effects models revealed a significant negative correlation between CP volume and WMH susceptibility value changes over time ($\beta = -0.274$, $P = 0.0296$). However, no significant relationship was found between CP volume and WMH volume changes ($\beta = 0.025$, $P = 0.936$) (Fig. 6). The pattern of cross-sectional and longitudinal findings suggests that susceptibility values may offer greater sensitivity in detecting disease progression than volumetric measurements do.

Random forest analysis

Random forest modeling revealed that the CP/ICV and WMH susceptibility values were significant predictors of CSVD severity (OOB-AUC = 0.698) (Fig. 7). These were the only two features confirmed by the Boruta algorithm as important predictors. Other variables, including A β 1–42, A β 1–40, A β 42/40, total tau, p-tau181, and the CP susceptibility value, were not retained as significant predictors in the model.

Discussion

This comprehensive study explored the intricate relationships between plasma amyloid markers, CP volume, and WMH characteristics (WMH volume and susceptibility) in CSVD participants using multimodal imaging and plasma biomarker analysis. Through cross-sectional and longitudinal analyses over a 20-month period, we assessed associations between CP volume, WMH characteristics, and plasma biomarkers to explore potential relationships that may suggest underlying pathways involved in CSVD progression. Our analyses revealed that plasma A β 1–40 levels were positively correlated with CP volume ($\beta = 0.115$, $P =$

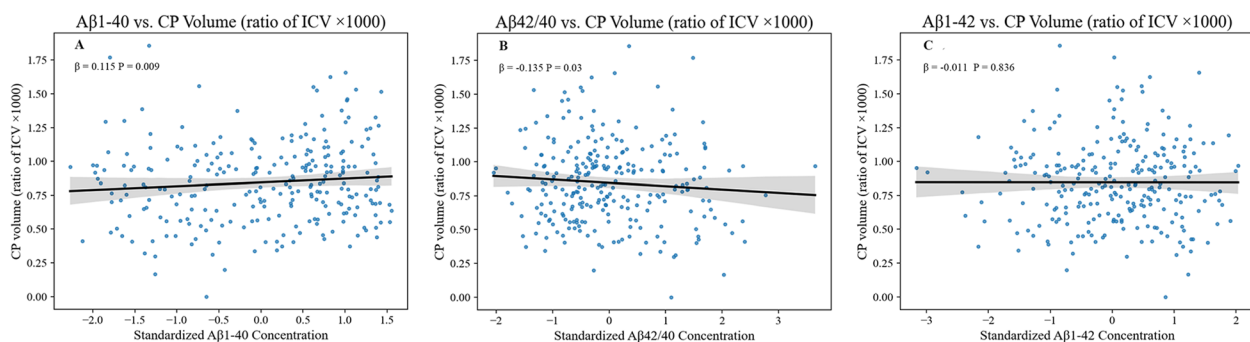


Fig. 4 Associations between plasma biomarkers and CP volume. This figure presents linear regression results for the associations between plasma biomarkers (A β 1–40, A β 42/40, and A β 1–42) and CP volume. **A** shows the association with A β 1–40, **B** with A β 42/40, and **C** with A β 1–42. Each plot includes the regression line and 95% confidence intervals. Regression coefficients and p values adjusted for age, sex, and education level are provided for each analysis. Abbreviations: CP = choroid plexus

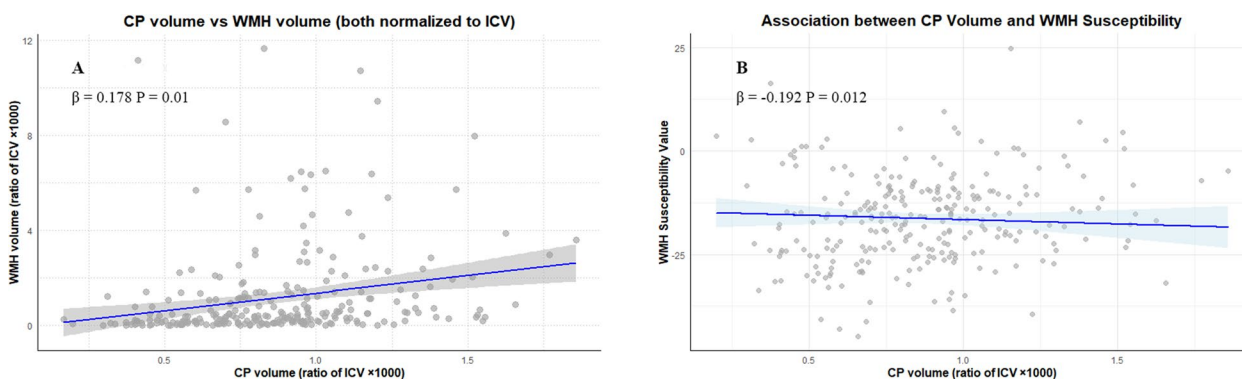


Fig. 5 Associations between CP volume, WMH volume, and WMH susceptibility. This figure shows the linear regression analyses investigating the relationships between CP volume and **(A)** baseline WMH volume and **(B)** WMH susceptibility. **A** Scatterplot showing the positive association between CP volume and baseline WMH volume. The regression model adjusts for age, sex, years of education, and lateral ventricle volume. **B** Scatterplot illustrating the correlation between CP volume and WMH susceptibility adjusted for the same covariates. For both panels, the blue regression lines represent the estimated relationships, with the shaded regions indicating the 95% confidence intervals. Abbreviations: CP = choroid plexus; WMH = white matter hyperintensity

0.009), whereas Aβ42–40 levels were inversely related ($\beta = -0.135, P = 0.03$), suggesting a specific pattern of amyloid–CP interactions. Increased CP volume was significantly associated with both WMH volume and WMH susceptibility values, as evidenced by increased WMH volume ($\beta = 0.191, P = 0.011$) and reduced WMH susceptibility ($\beta = -0.192, P = 0.012$). Notably, longitudinal analysis revealed that CP volume primarily influenced WMH susceptibility ($\beta = -0.274, P = 0.0296$) rather than volume changes over time ($\beta = 0.025, P = 0.936$), indicating that microstructural WMH alterations may precede volumetric changes. These findings suggest associations between CP volume, amyloid markers, and CSVD characteristics, which warrant further investigation into potential shared pathways. The inconsistent relationships between plasma amyloid

markers and CSVD severity noted in previous studies highlight the complexity of these interactions [12, 13]. Our data suggests that WMH susceptibility measurements may potentially serve as a sensitive marker for early CSVD monitoring.

Our finding of a nominally significant association between the Aβ42/40 ratio and WMH susceptibility, but not WMH volume, supports the notion that susceptibility measures may capture microstructural tissue alterations related to amyloid metabolism that precede volumetric changes. This observation aligns with our broader finding that CP volume changes were more consistently associated with WMH susceptibility than with WMH volume over time, reinforcing the potential utility of susceptibility mapping as a more sensitive marker for early white matter alterations in CSVD.

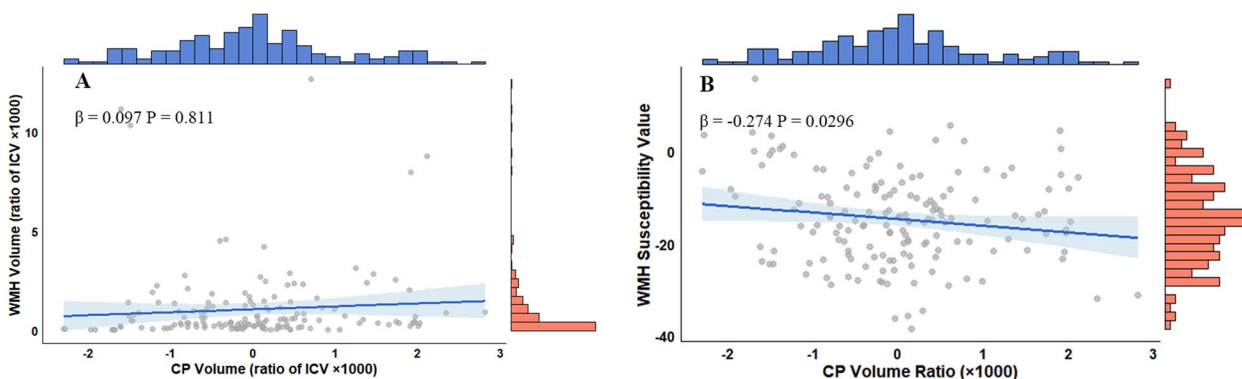


Fig. 6 Mixed-effects model analysis of the relationships between CP volume, WMH volume, and WMH susceptibility. This figure illustrates the longitudinal mixed-effects model results examining the associations between CP volume and **(A)** WMH volume and **(B)** WMH susceptibility. **A** Scatterplot depicting the relationship between CP volume and WMH volume. The mixed-effects model adjusts for age, sex, years of education, lateral ventricle volume, and follow-up duration as covariates. **B** Scatterplot showing the associations between CP volume and WMH susceptibility values adjusted for the same covariates. For both panels, the blue regression lines represent the fitted mixed-effects model predictions, with shaded regions indicating the 95% confidence intervals. Abbreviations: CP = choroid plexus; WMH = white matter hyperintensity

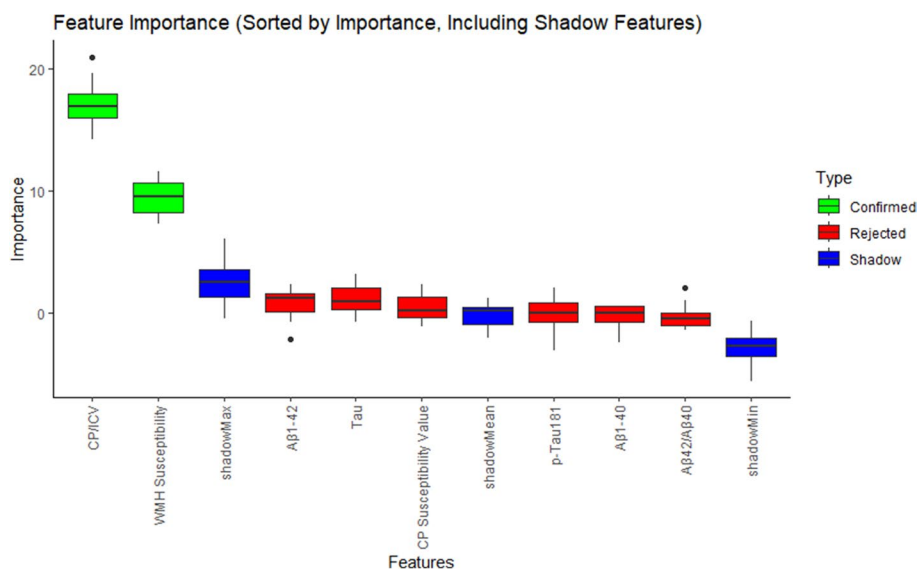


Fig. 7 Random forest informative predictors of CSVD. This figure displays the feature importance rankings derived from the Boruta algorithm, which are used to evaluate the contributions of various features in the prediction of CSVD severity. Features are categorized into three types, namely, confirmed (green), rejected (red), and shadow (blue), on the basis of their importance relative to shadow features. The boxplots represent the distribution of importance scores for each feature, with the y-axis indicating the feature importance and the x-axis listing the features. Boruta compares the importance of the original variables with the highest feature importance of the shadow features obtained via feature permuted copies. Poorly performing variables are progressively discarded. Compared with shadow features, confirmed features, such as CP/ICV and WMH susceptibility, demonstrate significantly greater importance. Rejected features have important scores that are comparable to or lower than those of shadow features. Shadow features serve as a baseline to assess the relevance of actual features. Abbreviations: CSVD = cerebral small vessel disease; CP/ICV = choroid plexus volume normalized to the intracranial volume; WMH = white matter hyperintensity

The relationship between amyloid markers and WMH susceptibility may be mediated through iron metabolism dysregulation and oxidative stress. Amyloid-beta is known to induce oxidative damage, potentially affecting iron-rich oligodendrocytes and triggering ferroptotic processes in microglia [20]. These cellular changes may alter tissue iron content and myelin integrity, which are sensitively detected by QSM. Recent research has specifically highlighted how amyloid deposition in cerebral vessels can disrupt vascular function, leading to hypoperfusion and subsequent white matter damage characteristic of CSVD [21]. The choroid plexus, serving as both a source of CSF production and an immune interface, may respond to these pathological processes by altering its volume to maintain brain homeostasis.

Our study revealed that plasma Aβ1-40 levels were significantly positively correlated with CP volume, whereas Aβ42-40 levels were negatively correlated with CP volume. The differential correlation pattern between CP volume and Aβ40 (positive) versus Aβ42 (no significant correlation) likely reflects fundamental differences in their clearance mechanisms. CP expresses transporters such as LRP1 and LRP2 that preferentially clear Aβ40 over Aβ42, as Aβ40 is more soluble and present in higher concentrations in CSF [22, 23]. The positive correlation between CP volume and Aβ40 may represent an adaptive response

enhancing clearance capacity, while the negative correlation with Aβ42/40 ratio further supports this interpretation. These findings are particularly relevant to CSVD pathology, as Aβ40 is the predominant component of vascular amyloid, while Aβ42 primarily deposits in brain parenchyma [24]. Elevated plasma Aβ40 levels have been associated with more severe WMH burden and lacunar infarcts [21]. Therefore, increased CP volume may initially represent a protective adaptation to enhance vascular amyloid clearance, but this compensatory mechanism may eventually become overwhelmed, leading to altered CSF dynamics and exacerbation of CSVD pathology [25].

Cross-sectional analysis revealed that increased CP volume was significantly associated with increased WMH volume and decreased susceptibility values. Studies have shown that changes in CP volume are key factors in the progression of CSVD [26]. Increased CP may cause metabolic abnormalities and an inflammatory response, promoting white matter damage. White matter contains abundant myelin produced by iron-rich oligodendrocytes, and decreased WMH susceptibility typically suggests reduced iron content or myelin loss [27]. Previous studies in diseases such as multiple sclerosis have shown that myelin loss and oligodendrocyte death are linked to changes in iron levels, as oligodendrocytes contain high levels of iron-storing proteins [28]. Therefore, reduced

WMH susceptibility values might indicate iron loss or redistribution, which is consistent with myelin damage and nerve fiber injury [29]. Notably, while CP volume had no significant effect on WMH volume over time, its relationship with WMH susceptibility remained significant during follow-up, suggesting that WMH susceptibility might better reflect CSVD progression.

Our random forest model identified CP volume and WMH susceptibility values as the most important indicators for determining CSVD severity, further supporting the crucial role of CP in CSVD progression. WMH susceptibility values reveal additional subtle white matter changes that go beyond traditional volume assessments. The predictive value of CP volume indicates its important role in brain health, which may directly shape CSVD development. These findings support the potential use of CP volume as an early marker for monitoring disease progression.

Our analysis revealed that plasma A β 1–40 was significantly correlated with CP volume, whereas A β 42–40 was negatively associated with CP volume [30]. However, our random forest model did not identify either of these plasma biomarkers as significant variables for discriminating CSVD severity. Additionally, mediation analysis revealed no direct relationship between A β levels and CSVD severity. These results indicate that plasma amyloid markers correlate with CP volume but were not identified as direct predictors of CSVD severity in our analysis. This suggests any influence of amyloid markers on CSVD manifestations may occur through indirect mechanisms, possibly involving CP structural alterations. This finding aligns with the inconsistent relationships between amyloid markers and CSVD reported in previous studies [12, 13], highlighting the complex interplay between amyloid metabolism, CP function, and cerebrovascular pathology. Our findings suggest that the CP mediates the interaction between systemic amyloid markers and cerebrovascular alterations in patients with CSVD. This observation aligns with established evidence showing that the CP regulates molecular exchange between the blood and the CNS [31]. The CP not only responds to systemic signals but also modulates the brain environment by regulating A β clearance, CSF composition, and flow patterns [7]. Understanding this mediating role of CP could be particularly important for developing therapeutic strategies that target CP-mediated pathways in CSVD progression.

This study has several limitations. First, our relatively limited longitudinal data and short follow-up period restrict our understanding of long-term CSVD progression. Second, we lacked a dedicated healthy control group, using the CSVD(0) group as an internal reference instead. While we controlled for age in our analyses, future studies should incorporate well-matched healthy controls to better determine whether

CP volume changes are specifically related to CSVD pathology or represent normal aging variations. Third, our imaging protocol was not optimized to distinguish between CSVD subtypes (arteriolosclerotic CSVD vs. cerebral amyloid angiopathy). Future studies should incorporate advanced techniques like SWI for precise microbleed localization, along with amyloid PET or CSF biomarkers, to explore subtype-specific CP alterations. Finally, while we found a nominally significant association between the A β 42/40 ratio and WMH susceptibility ($p = 0.040$), this result did not survive correction for multiple comparisons and should be interpreted cautiously. Nevertheless, it provides preliminary evidence that susceptibility measurements may detect subtle amyloid-related tissue changes not captured by conventional volumetric analyses. Future research should validate these relationships in larger multicenter cohorts with extended follow-up periods. As high-resolution MRI techniques advance, combining CP structural and functional analyses may reveal more comprehensive associations between CSF circulation and cerebrovascular health, potentially providing promising biomarkers for CSVD diagnosis and intervention.

Conclusions

CP volume changes significantly correlated with both WMH volume and WMH susceptibility in CSVD patients, with WMH susceptibility serving as a more sensitive early marker of CP-related white matter changes. The strong associations between plasma amyloid markers and CP volume, along with the identification of CP volume as a key predictor of CSVD severity, suggest that CP-mediated pathways may represent an important link between amyloid metabolism and CSVD progression.

Supplementary Information

The online version contains supplementary material available at <https://doi.org/10.1186/s13195-025-01740-8>.

Supplementary Material 1.

Acknowledgements

The author expresses gratitude to all the participants of this study and their families for their selfless dedication.

Authors' contributions

L.P. wrote the main manuscript text. L.M. prepared the imaging data. L.P. prepared figures and tables. G.L. prepared the clinical data. L.C. and L.J. revised the text and polished the language. G.L., C.Y., C.Z., Z.X., Z.N., W.N., and W.Y. contributed to the acquisition of data. All the authors reviewed the manuscript.

Funding

This work was supported by grants from the National Natural Science Foundation of China (82272072), the Natural Science Foundation of Shandong Province (ZR2020MH288, ZR2024MH026), the Technology Development Plan of Jinan (202328066), the Medical and Health Science and Technology Development Project of Shandong Province (202309010557, 202309010560, 202409010479).

Data availability

No datasets were generated or analysed during the current study.

Declarations**Ethics approval and consent to participate**

All study procedures were approved by the Ethical Committee of the Institutional Review Board (IRB) of the Shandong Institute of Medical Imaging (2019–002). The study was conducted in accordance with the Declaration of Helsinki. All participants signed an informed consent form before the commencement of the study.

Consent for publication

Not applicable.

Competing interests

The authors declare no competing interests.

Author details

¹Key Laboratory of Endocrine Glucose & Lipids Metabolism and Brain Aging, Ministry of Education; Department of Radiology, Shandong Provincial Hospital Affiliated to Shandong First Medical University, 324 Jing-Wu Road, Jinan, Shandong 250021, China. ²Department of Psychiatry and Psychotherapy, Jena University Hospital, Philosophenweg 3, Jena 07743, Germany. ³Binzhou Medical University, China. Guanhai Road No.346, Yantai, Shandong 264003, China. ⁴Department of Radiology, Beijing Tsinghua Changgung Hospital, School of Clinical Medicine, Tsinghua Medicine, Tsinghua University, 168 Litang Road, Changping District, Beijing 102218, China.

Received: 28 December 2024 Accepted: 14 April 2025

Published: 23 April 2025

References

- Wardlaw JM, Smith C, Dichgans M. Small vessel disease: mechanisms and clinical implications. *The Lancet Neurology*. 2019;18:684–96.
- Smith EE, Biessels GJ, De Guio F, de Leeuw FE, Duchesne S, Düring M, et al. Harmonizing brain magnetic resonance imaging methods for vascular contributions to neurodegeneration. *Alzheimer's & dementia (Amsterdam, Netherlands)*. 2019;11:191–204.
- Debette S, Schilling S, Duperron M-G, Larsson SC, Markus HS. Clinical Significance of Magnetic Resonance Imaging Markers of Vascular Brain Injury: A Systematic Review and Meta-analysis. *JAMA Neurol*. 2019;76:81–94.
- Sweeney MD, Kisler K, Montagne A, Toga AW, Zlokovic BV. The role of brain vasculature in neurodegenerative disorders. *Nat Neurosci*. 2018;21:1318–31.
- Brown R, Benveniste H, Black SE, Charpak S, Dichgans M, Joutel A, et al. Understanding the role of the perivascular space in cerebral small vessel disease. *Cardiovasc Res*. 2018;114:1462–73.
- Lun MP, Monuki ES, Lehtinen MK. Development and functions of the choroid plexus–cerebrospinal fluid system. *Nat Rev Neurosci*. 2015;16:445–57.
- Tadayon E, Pascual-Leone A, Press D, Santarnecchi E. Choroid plexus volume is associated with levels of CSF proteins: relevance for Alzheimer's and Parkinson's disease. *Neurobiol Aging*. 2020;89:108–17.
- Choi JD, Moon Y, Kim H-J, Yim Y, Lee S, Moon W-J. Choroid Plexus Volume and Permeability at Brain MRI within the Alzheimer Disease Clinical Spectrum. *Radiology*. 2022;304:635–45.
- Margoni M, Gueye M, Meani A, Pagani E, Moiola L, Preziosa P, et al. Choroid plexus enlargement in paediatric multiple sclerosis: clinical relevance and effect of sex. *J Neurol Neurosurg Psychiatry*. 2023;94:181–8.
- Yao Y, Nguyen TD, Pandya S, Zhang Y, HurtadoRúa S, Kovanlikaya I, et al. Combining Quantitative Susceptibility Mapping with Automatic Zero Reference (QSM0) and Myelin Water Fraction Imaging to Quantify Iron-Related Myelin Damage in Chronic Active MS Lesions. *AJNR Am J Neuroradiol*. 2018;39:303–10.
- Kwak SS, Washicosky KJ, Brand E, Von Maydell D, Aronson J, Kim S, et al. Amyloid- β 42/40 ratio drives tau pathology in 3D human neural cell culture models of Alzheimer's disease. *Nat Commun*. 2020;11:1377.
- Roseborough A, Ramirez J, Black SE, Edwards JD. Associations between amyloid β and white matter hyperintensities: A systematic review. *Alzheimers Dement*. 2017;13:1154–67.
- Saridin FN, Hilal S, Villaraza SG, Reilhac A, Gyanwali B, Tanaka T, et al. Brain amyloid β , cerebral small vessel disease, and cognition: A memory clinic study. *Neurology*. 2020;95:e2845–53.
- Čarna M, Onyango IG, Katina S, Holub D, Novotny JS, Nezvedova M, et al. Pathogenesis of Alzheimer's disease: Involvement of the choroid plexus. *Alzheimers Dement*. 2023;19:3537–54.
- Klarenbeek P, van Oostenbrugge RJ, Rouhi RPW, Knottnerus ILH, Staals J. Ambulatory blood pressure in patients with lacunar stroke: association with total MRI burden of cerebral small vessel disease. *Stroke*. 2013;44:2995–9.
- Al Amin Olama A, Wason JMS, Tuladhar AM, van Leijssen EMC, Koini M, Hofer E, et al. Simple MRI score aids prediction of dementia in cerebral small vessel disease. *Neurology*. 2020;94:e1294–302.
- Fazekas F, Chawluk JB, Alavi A, Hurlst H, Zimmerman RA. MR signal abnormalities at 1.5 T in Alzheimer's dementia and normal aging. *AJR Am J Roentgenol*. 1987;149:351–6.
- Esteban O, Markiewicz CJ, Blair RW, Moodie CA, Isik AI, Erramuzpe A, et al. fMRIprep: a robust preprocessing pipeline for functional MRI. *Nat Methods*. 2019;16:111–6.
- Müller J, Sinnecker T, Wendebourg MJ, Schläger R, Kuhle J, Schädelin S, et al. Choroid Plexus Volume in Multiple Sclerosis vs Neuromyelitis Optica Spectrum Disorder: A Retrospective, Cross-sectional Analysis. *Neuroimmunol Neuroinflamm*. 2022;9:e1147.
- Everett J, Brooks J, Lermyte F, O'Connor PB, Sadler PJ, Dobson J, et al. Iron stored in ferritin is chemically reduced in the presence of aggregating A β (1–42). *Sci Rep*. 2020;10:10332.
- van Leijssen EMC, Kuiperij HB, Kersten I, Bergkamp MI, van Uden IWM, Vanderstichele H, et al. Plasma A β (Amyloid- β) Levels and Severity and Progression of Small Vessel Disease. *Stroke*. 2018;49:884–90.
- Crossgrove JS, Li GJ, Zheng W. The Choroid Plexus Removes β -Amyloid from Brain Cerebrospinal Fluid. *Exp Biol Med (Maywood)*. 2005;230:771–6.
- González-Marrero I, Giménez-Llort L, Johanson CE, Carmona-Calero EM, Castañeyra-Ruiz L, Brito-Armas JM, et al. Choroid plexus dysfunction impairs beta-amyloid clearance in a triple transgenic mouse model of Alzheimer's disease. *Front Cell Neurosci*. 2015;9:17.
- Yamada M, Hamaguchi T, Sakai K. Acquired cerebral amyloid angiopathy: An emerging concept. *Prog Mol Biol Transl Sci*. 2019;168:85–95.
- Jeong SH, Park CJ, Cha J, Kim S-Y, Lee S-K, Kim YJ, et al. Choroid Plexus Volume, Amyloid Burden, and Cognition in the Alzheimer's Disease Continuum. *Aging Dis*. 2024;16:552–64.
- Li C, Zhang H, Wang J, Han X, Liu C, Li Y, et al. Choroid Plexus Volume in Rural Chinese Older Adults: Distribution and Association With Cardiovascular Risk Factors and Cerebral Small Vessel Disease. *JAMA*. 2024;13:e035941.
- Zhang Y, Gauthier SA, Gupta A, Chen W, Comunale J, Chiang GC-Y, et al. Quantitative Susceptibility Mapping and R2* Measured Changes during White Matter Lesion Development in Multiple Sclerosis: Myelin Breakdown, Myelin Debris Degradation and Removal, and Iron Accumulation. *AJNR Am J Neuroradiol*. 2016;37:1629–35.
- Adeniyi PA, Gong X, MacGregor E, Degener-O'Brien K, McClendon E, Garcia M, et al. Ferroptosis of Microglia in Aging Human White Matter Injury. *Ann Neurol*. 2023;94:1048–66.
- Bartzokis G, Lu PH, Tishler TA, Fong SM, Oluwadara B, Finn JP, et al. Myelin Breakdown and Iron Changes in Huntington's Disease: Pathogenesis and Treatment Implications. *Neurochem Res*. 2007;32:1655–64.
- Bouhara M, Walker KA, Alisch JSR, Gong Z, Mazucanti CH, Lewis A, et al. Association of Plasma Markers of Alzheimer's Disease, Neurodegeneration, and Neuroinflammation with the Choroid Plexus Integrity in Aging. *Aging Dis*. 2024;15:2230–40.
- Strazielle N, Mutin M, Ghersi-Egea JF. Les plexus choroïdes : une interface dynamique entre sang et liquide céphalo-rachidien. *Morphologie*. 2005;89:90–101.

Publisher's Note

Springer Nature remains neutral with regard to jurisdictional claims in published maps and institutional affiliations. We sincerely thank Dr. Yuan Cao for her invaluable contribution to the development of the automated choroid plexus segmentation pipeline, which significantly improved the accuracy of our methodology.